

5.1 UNDERSTANDING THE VALUE OF HIGH RESOLUTION REGIONAL CLIMATE MODELING

James M. Done* L. Ruby Leung², Christopher A. Davis¹ and Bill Kuo¹

1. National Center for Atmospheric Research, Boulder, CO

2. Pacific Northwest National Laboratory, Richland, WA

1 INTRODUCTION

A regional climate model (RCM) provides high resolution climate scenarios important for impact assessment and resource management. High resolution allows for a more precise description of regional topographic forcings due to orography, land-sea contrasts and vegetation characteristics. Consequently, processes strongly forced by topography, such as orographic precipitation and monsoon circulations, improve at increased resolution (Giorgi and Marinucci, 1996). Since better resolved small-scale processes may have improved large-scale impacts, RCMs can be used to study the upscale impact of regional forcings (e.g. the orographic shadowing effect) on the large-scale climate, in addition to climate downscaling. With increasing computational power that enables global climate models to be applied at higher spatial resolution, it is important to assess the value of higher resolution (1 - 10km grid-spacing) regional climate modeling. Higher resolution does not necessarily imply more accurate climate simulation (e.g. Boyle (1993), Sperber *et al.* (1994) and Senior (1995)). The sensitivity of physics parameterizations to model grid-spacing may overwhelm any benefits of higher resolution simulation (Duffy *et al.*, 2003). There are also fundamental differences in how the solutions of short-term forecast models and RCMs depend on resolution.

The Weather Research and Forecasting (WRF) model (Michalakes *et al.*, 2001) is designed specifically for high-resolution limited-area applications. The model uses high order numerical accuracy to solve the fully compressible non-hydrostatic equations, and therefore provides a suitable tool to understand the value of high resolution (1 - 10km grid-spacing) regional climate modeling. This study builds on previous regional climate research using the fifth-generation Pennsylvania State University-NCAR mesoscale model (MM5) (Leung *et al.*, 2003, Leung and Qian, 2003), and represents the first step in assessing the value of high resolution (1-10km grid spacing) regional climate modeling using version 2 of the WRF model.

Model evaluation concentrates on the region of the western United States where topographic forcings play an important role in defining the regional climate, and where it is thought high resolution regional climate mod-

* Corresponding author address: James M. Done, National Center for Atmospheric Research, P.O. Box 3000, Boulder, CO 80307, USA ; e-mail: done@ucar.edu



Figure 1: Regional climate model domains: WRF30 (parent) and WRF6 (nested).

eling will have the greatest impact. Since water resources in this region is derived largely from cold season precipitation and snowpack, and accurate regional climate models are important in providing climate scenarios for impact assessment and resource management, our preliminary model evaluation concentrates on precipitation, snowpack and 2m temperature.

2 METHODOLOGY

Simulations of the cold-season regional climate of the western United States are performed at 30km and 6km horizontal grid spacings (hereafter, WRF30 and WRF6 respectively) using a one-way nested configuration. Both domains use 31 vertical sigma levels. The parent domain of 125×150 grid points, shown in Fig. 1, includes the major river basins of the Columbia, Colorado and Sacramento rivers, and extends far enough south to allow simulation of the warm-season North American Monsoon climate (not presented here). The nested domain of 111×126 grid points covers the Pacific Northwest region as shown in Fig. 1. The terrain fields for both WRF6 and WRF30 are shown in Fig. 2 for the region of the WRF6 domain. The fields include terrain features on the smallest resolvable scales of the model resulting in a more precise description of topography at smaller grid-spacing.

Simulations run for 4 months from 1st October 1990

through 31st January 1991. For the parent domain (WRF30), initial, lateral and lower boundary conditions are derived from the NCEP-NCAR reanalyses at 2.5° horizontal grid spacing interpolated onto the WRF model grid. Solutions on the parent domain provide lateral boundary conditions for the nested domain. Relaxation at all boundaries has a combined linear/exponential functional form over 10 grid points, and lateral boundary conditions are updated every 6 hours. To aid long-term integrations the lower boundary conditions of sea surface temperature, vegetation fraction and albedo are updated every 6 hours.

The same physics parameterizations are used for both domains: boundary and surface-layer processes are represented by the Monin-Obukhov (Janjic Eta) surface scheme, the Noah land surface model and the Mellor-Yamada-Janjic (Eta) TKE boundary layer scheme; convection is parameterized by the Eta Kain-Fritsch scheme; explicit precipitation processes are parameterized by the Ferrier scheme; radiation is represented by the rapid radiative transfer model and the Dudhia short-wave scheme.

Two datasets are used to analyze the regional climate of the western United States. The first consists of daily rainfall amount and daily maximum and minimum 2m temperature gridded at $1/24^\circ$ (approximately 4.4km), developed by C. Daly and W. Gibson of the Spatial Climate Analysis Service at Oregon State University and G. Taylor of the Oregon Climate Service at Oregon State University. This dataset is available at <http://www.ocs.orst.edu/prism/docs/meta/>. A statistical topographic-precipitation relationship developed by Daly *et al.* (1994) is used to spatially interpolate the station observations to capture the mesoscale details of precipitation distribution in regions of complex terrain.

The second dataset consists of daily snow water equivalent, 2m temperature and rainfall totals at the snowpack telemetry (snotel) stations in the western United States. There are a total of about 650 snotel stations typically located in remote mountain sites; with 83 snotel stations located within the WRF6 domain as shown in Fig. 2.

3 RESULTS

Precipitation

The WRF30 average daily precipitation amount agrees well with observations in terms of spatial distribution, as shown in Fig. 3. In agreement with 40km MM5 simulations by Leung and Qian (2003), WRF30 shows a lack of precipitation along the coastal hills, good simulation over the Cascade Range and a slight overprediction over the basins beyond. The WRF30 barrier height for the coastal hills is about half that at $1/24^\circ$ grid-spacing (not shown) resulting in reduced topographic forcing and precipitation amounts are underpredicted, whereas for the larger scale Cascade Range the barrier height is more accurate and precipitation amounts are well simulated.

As expected the WRF6 precipitation field, shown in Fig. 3, shows finer-scale structure associated with finer-scale topographic forcing. The WRF6 precipitation also shows increased range in magnitude east-west across terrain maxima. A comparison with the $1/24^\circ$ observations interpolated onto the WRF6 grid indicates the fine-scale structure is realistic, but shows that WRF6 overestimates precipitation over the western slopes of the Cascade Range, yet underestimates precipitation over the coastal hills and over the low-lying areas between the coastal hills and the Cascades. The rain shadow effect in the lee of the Cascade Range is weaker in WRF30 than observed, but is much improved in WRF6.

Temperature

The WRF30 cold-season average 2m temperature compares well with observations in terms of spatial distribution and magnitude, as shown in Fig. 4. The range in magnitude is slightly less for WRF30 than observed. The WRF6 cold-season average 2m temperature, shown in Fig. 4, shows finer-scale structure associated with finer-scale topography, and also shows increased range in magnitude. A comparison with the $1/24^\circ$ observations interpolated onto the WRF6 grid shows this fine-scale structure to be realistic. In contrast to WRF30, the WRF6 2m temperature shows a warm bias of up to 1.5°C over the basins in the lee of the Cascade Range. Both WRF30 and WRF6 show cool biases over the northern Cascades and warm biases over the southern Cascades; possibly related to snow cover (see next section).

Snowpack

Decreased grid-spacing has a dramatic impact on simulated snowpack (snow water equivalent). The maximum cold-season average snowpack in WRF30 is 0.19m compared to 1.73m in WRF6. For both WRF30 and WRF6, snowpack accumulates where 2m temperatures are low and where precipitation is significant (not shown). Fig. 5 shows WRF30 snowpack confined to the northern half of the Cascade Range, whereas snowpack in WRF6 extends across parts of the southern Cascade Range and eastern Oregon State. Snowpack in WRF6 has much higher amplitude of variability associated with the more precise description of terrain and finer-scale details of temperature and precipitation.

A comparison of WRF6, WRF30 and observed snowpack at the locations of 83 snotel stations within the WRF6 domain, shown in Fig. 6, shows snowpack simulation is very poor, and indicates that increased model resolution brings only a slight improvement. The snotel station average snowpack for WRF30, WRF6 and observations is 11mm, 15mm and 141mm respectively.

Despite the more accurate station elevations in WRF6 (see Fig. 6), the station average 2m temperature biases for WRF30 and WRF6 are similar at $+1^\circ\text{C}$ and $+0.8^\circ\text{C}$ respectively, and the correlations between observations and model simulations are generally poor. The model also underpredicts precipitation amounts at the

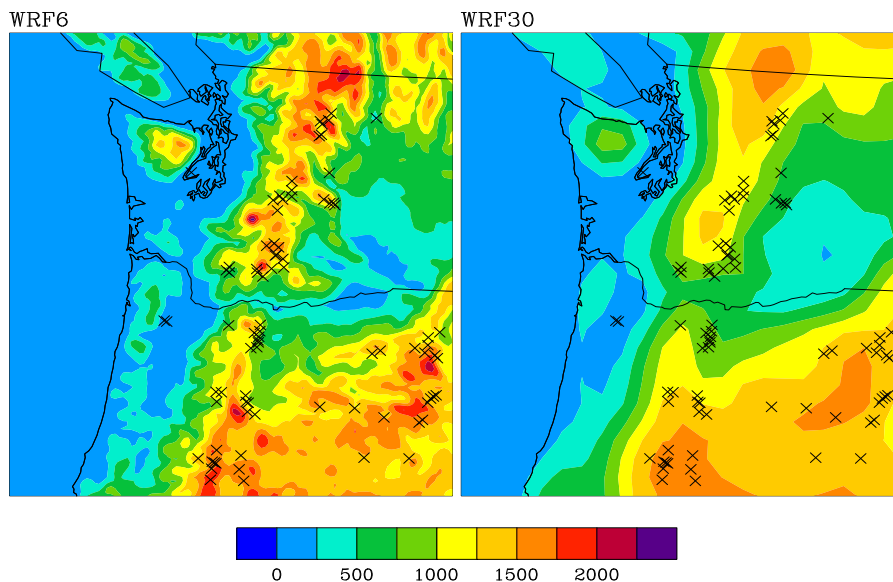


Figure 2: Terrain height (m) for WRF6 and WRF30 for the region of the WRF6 domain. Crosses mark the locations of 83 snotel stations.

snotel sites. The station average daily mean precipitation totals for WRF30, WRF6 and observations are 4.7mm, 3.3mm and 7.3mm respectively.

Snotel stations are generally located below maxima in terrain features and close to the WRF6 snow-line (see Fig. 5). In addition, the majority of stations are located on the eastern slopes of terrain maxima (see Fig. 2); the opposite side to WRF6 precipitation maxima (see Fig. 3). The positive temperature bias and negative precipitation bias will contribute to poor snowpack simulation; however, snowpack may be more sensitive to details of the Noah land surface model.

4 CONCLUSIONS

A high resolution regional climate simulation showed realistic small-scale spatial variability of precipitation and 2m temperature. Substantial increases in cold-season average snowpack occurred locally on using smaller grid-spacing, yet biases in temperature and precipitation and the details of the land surface model may have resulted in the poor comparison with observations at selected observing stations.

Locally, the long-term simulation of precipitation and snowpack were highly sensitive to the regional climate model grid-spacing. Analysis is in progress to determine the sensitivity of precipitation and snowpack over larger areas to model grid-spacing which has implications for regional hydrological modeling.

5 FUTURE WORK

A more detailed evaluation of cold-season simulations is needed to further understand the value of high resolution regional climate modeling. In particular, the topography-precipitation and temperature-precipitation-snowpack re-

lationships will be examined in more detail. Averages of seasonal simulations over a few years will determine the robustness of the preliminary results.

Attention will then focus on understanding the impact of high resolution regional climate modeling on the warm-season North American Monsoon climate. The monsoon climate will be evaluated based on the observational dataset described in this study and North American Monsoon Experiment (NAME) radar composites. Simulations at 4km grid-spacing, without a parameterization of convection, will be compared to a simulations using 30km grid-spacing.

Finally, rather than using RCMs for downscaling climate information, their real value may lies in the ability to study the interaction between regional topographic forcings and the large-scale climate signal. This study has indicated there may be improvements to the large-scale climate signal using high resolution RCMs, evidenced by the improved rain shadow effect in the lee of the Cascade Range. More work is needed to establish the validity of the WRF model for high resolution long-term simulation for both upscaling and downscaling research.

ACKNOWLEDGEMENTS. We thank Wei Wang and Jimy Dudhia for assistance with the WRF model. This work is supported by the NCAR FY04 opportunity fund.

REFERENCES

- Boyle, J. (1993). Sensitivity of dynamical quantities to horizontal resolution for a climate simulation using the ECMWF(cycle 33) model. *J. Climate*, **6**, 796–815.
- Daly, C., Neilson, R., and Phillips, D. (1994). A statistical-topographic model for mapping climatolog-

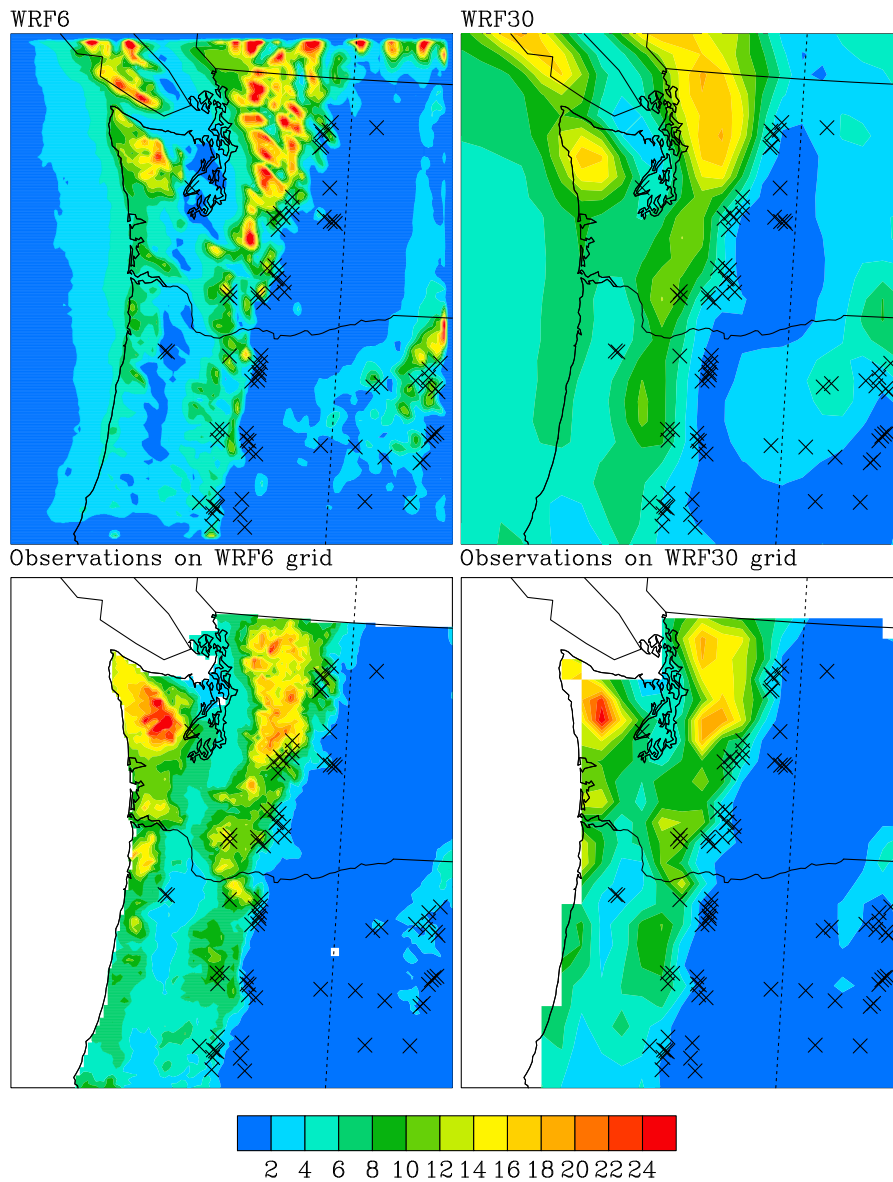


Figure 3: Daily average precipitation amount (mm) for WRF6, WRF30 and observations interpolated from the 1/24° grid onto the WRF6 and WRF30 grids. The crosses mark the locations of 83 snotel stations.

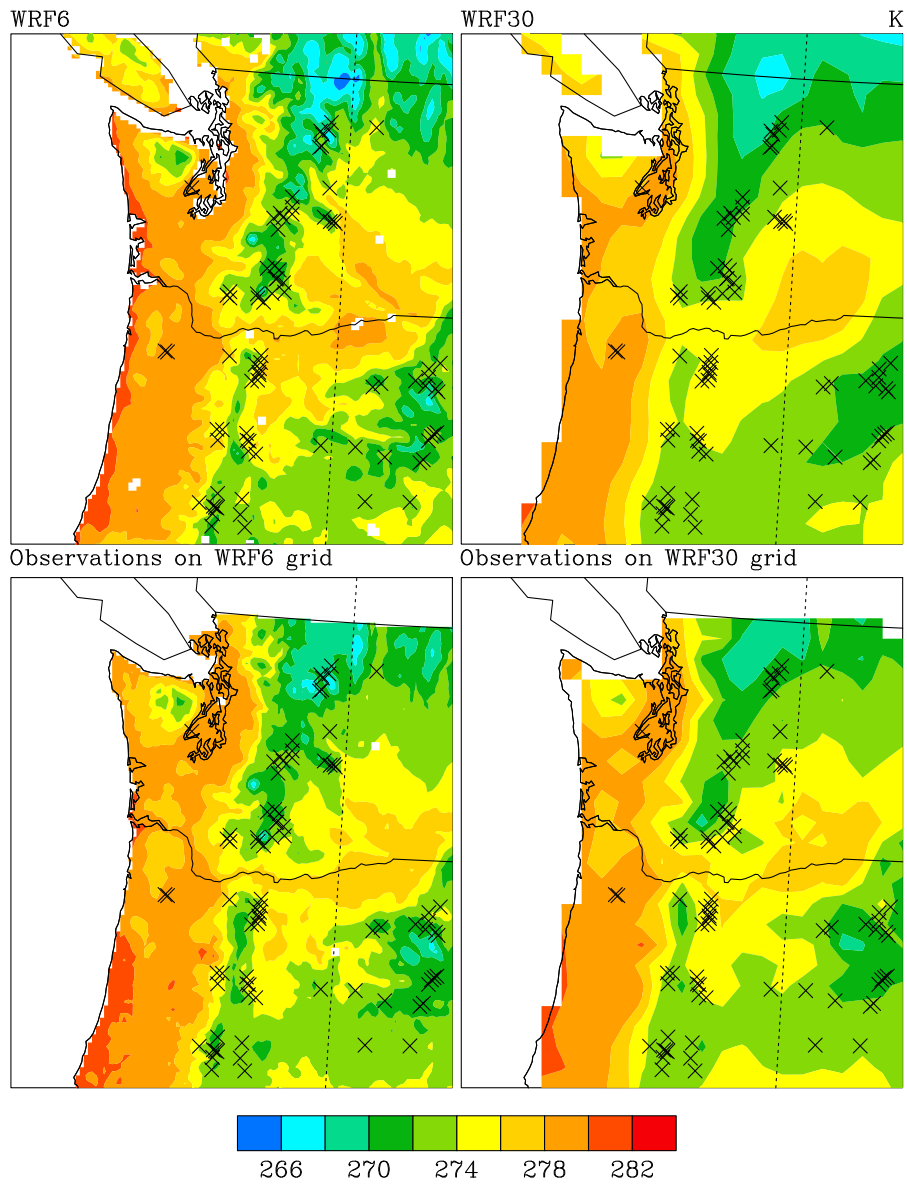


Figure 4: Cold-season average 2m temperature (K) for WRF6, WRF30 and observations interpolated from the $1/24^\circ$ grid onto the WRF6 and WRF30 grids. Crosses mark the locations of 83 snotel stations.

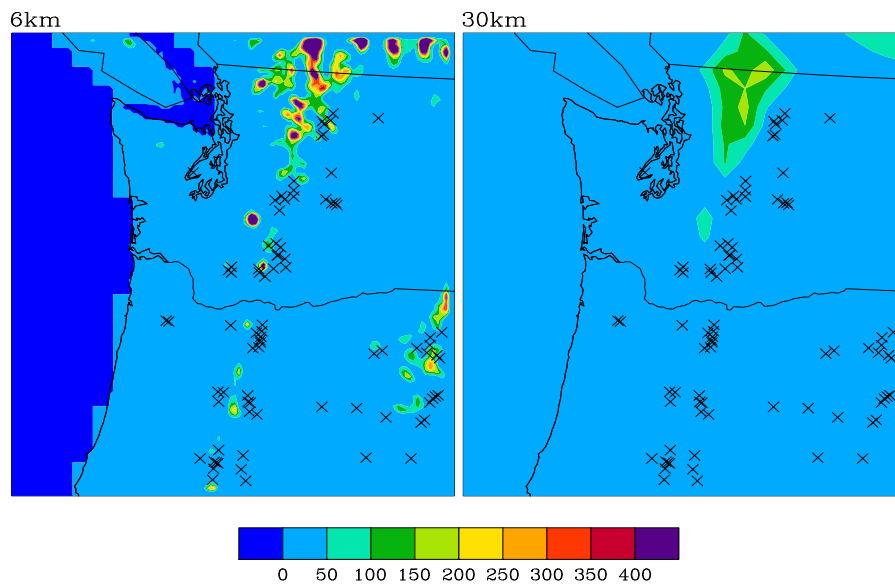


Figure 5: Cold-season average snowpack (snow water equivalent) (mm) for WRF6 and WRF30. Crosses mark the locations of 83 snotel stations.

ical precipitation over mountainous terrain. *J. Appl. Meteor.*, **33**, 140–158.

Duffy, P., Govindasamy, B., Iorio, J., Milovich, J., Sperber, K., Taylor, K., Wehner, M., and Thompson, S. (2003). High resolution simulations of global climate. Part I: Present climate. *Climate Dyn.*, **21**, 371–390.

Giorgi, F. and Marinucci, M. (1996). An investigation of the sensitivity of simulated precipitation to model resolution and its implications for climate studies. *Mon. Wea. Rev.*, **124**, 148–166.

Leung, L. and Qian, Y. (2003). The sensitivity of precipitation and snowpack simulations to model resolution via nesting in regions of complex terrain. *J. Hydrometeorol.*, **4**, 1025–1043.

Leung, L., Qian, Y., and Bian, X. (2003). Hydroclimate of the western United States based on observations and regional climate simulation of 1981–2000. Part I: Seasonal statistics. *J. Climate*, **16**, 1892–1911.

Michalakes, J., Chen, S., Dudhia, J., Hart, L., Klemp, J., Middlecoff, J., and Skamarock, W. (2001). Development of a next generation regional weather research and forecast model. In *Developments in Teracomputing: Proceedings of the Ninth ECMWF Workshop on the Use of High Performance Computing in Meteorology*, Zweiflhofer W, Krietz N(eds). World Scientific: Singapore.

Senior, C. (1995). The dependence of climate sensitivity on the horizontal resolution of a GCM. *J. Climate*, **8**, 2860–2880.

Sperber, K., Hameed, S., Potter, G., and Boyle, J. (1994). Simulation of the northern summer monsoon in the ECMWF model: Sensitivity to horizontal resolution. *Mon. Wea. Rev.*, **122**, 2461–2481.

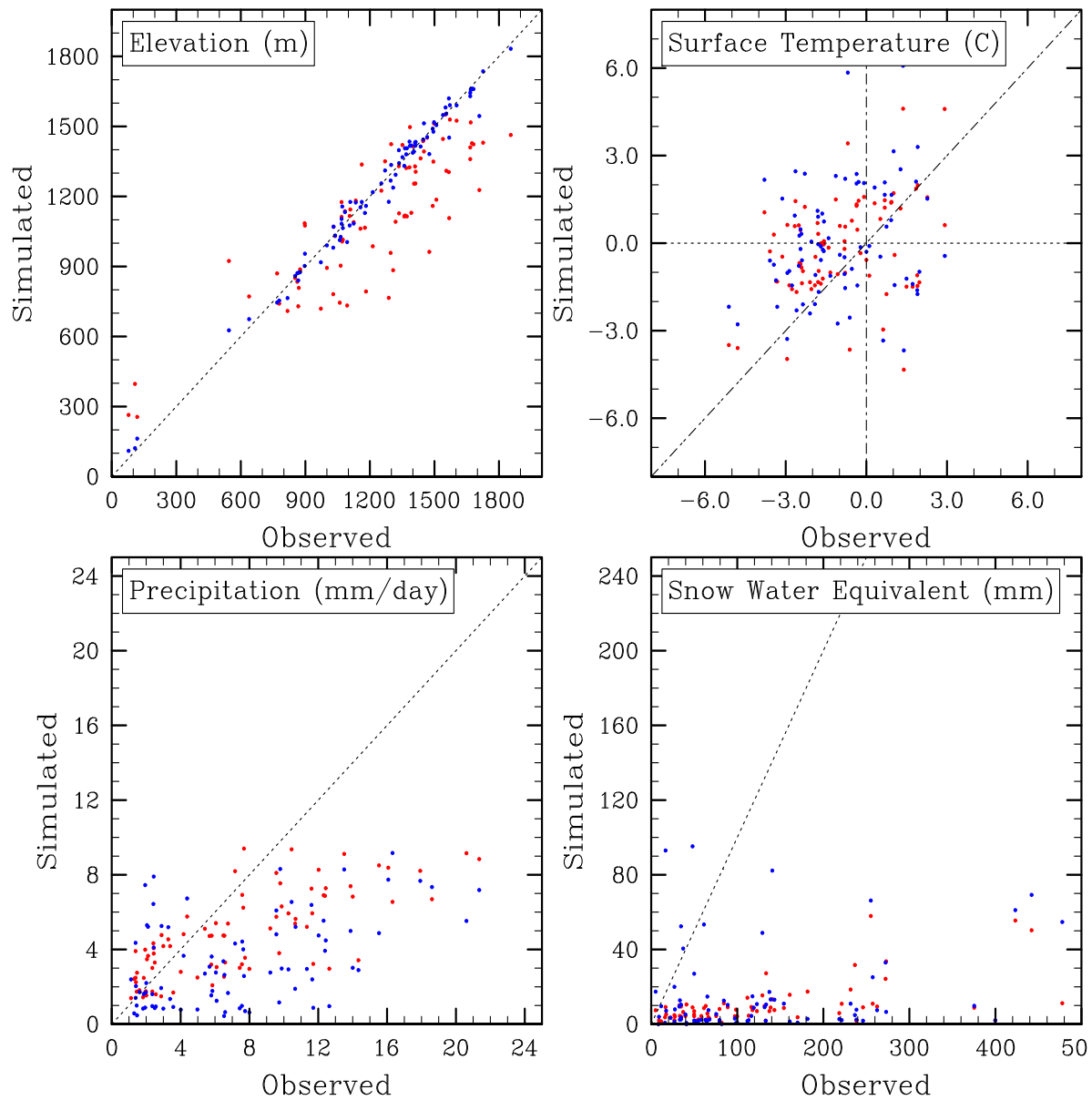


Figure 6: Scatter plots of observed and simulated surface variables at the locations of 83 snotel stations within the WRF6 domain for WRF6 (blue) and WRF30 (red).